International Journal of Applied Engineering Research ISSN 0973-4562 Volume 19, Number 4 (2024) pp. 407-414

A comparative study of ZnO-SiO_2 nano-composite and ZnO thin films for application as a buffer layer in CIGS solar cell

Rajni Seth
Department of Physics, Dyal Singh College, Karnal

Abstract
The present study reports the synthesis of ZnO and ZnO-SiO_2 nano-composite thin films using chemical bath deposition process for its application as a buffer layer in thin film CIGS solar cell. Comparison of optical, structural and morphological characteristics of ZnO thin films with ZnO-SiO_2 nano-composite thin film is reported. The size of the nano-crystallites varied between 1.7 nm and 1.8nm for both the samples. It was observed that use of TEOS as a surface modifier helped in reducing the deposition time. Addition of silica improved the optical characteristics of ZnO in the visible region and also increased the material coverage on the substrate. The transmittance of composite thin film is observed to be higher (95%) as compared to that of pure ZnO (92.9%) whereas values of refractive index as well as dielectric constant are found to be decreased. The lower and constant value of extinction coefficient of ZnO-SiO_2 nano-composite thin films as compared to ZnO is reported. Sheet resistance of ZnO-SiO_2 thin film ($2.958x10^8\Omega$/square) is decreased as compared to pure ZnO thin film($8.1x10^8\Omega$/square). XRD analysis showed that both the samples were amorphous.
Key Words: nano-composite thin film, buffer layer, TEOS, optical characteristics, Sheet resistance

1. Introduction

Owing to high emission level of greenhouse gases namely carbon dioxide, carbon monoxide, sulphur dioxide, phosphorous pentoxide and acidification caused by the traditional fossil fuels, the search for renewable sources of energy is a major thrust area as an alternative to conventional energy sources. Moreover the cost of using non-renewable energy is increasing drastically. The social and environmental costs, such as the cost for reliable oil supplies, processing of nuclear wastes, and the expenditure incurred during the disaster relief operations are increasing rapidly. So, there is need to replace these conventional sources with non-conventional one. Solar energy is generally believed to be the most clean and sustainable energy source and its judicious use has gained paramount importance in the present scenario. To make solar cells with higher efficiencies, new materials and concepts for development of solar cell devices are being exploited. Traditional solar cells are costly as complicated, high temperature and vacuum based techniques are often employed for their fabrication. In order to overcome such difficulties associated with the traditional solar cells, researchers came forward to develop flexible thin film solar cells and solar pastes. Thin film solar cells exhibit several advantages over crystalline silicon cells. These cells are light-weight, flexible, durable and stable. The quantity of materials required for fabrication of a thin film solar cell is less because it consists of layers of a few micrometres. Thus impurities and crystal defects may be avoided to a large extent as compared to that of crystalline silicon. Surface of a thin film can be improved to achieve desired optical characteristics. In case of multi component materials, compositions and band gap can be tuned by monitoring the crystallite size. While using thin film technology, it is easier to join individual solar cells to form large modules which can further be integrated through manufacturing processes for device applications. Moreover, as the quantity of material used is less as compared to silicon solar cells; energy payback period reduces. Most of the thin film deposition techniques are ecofriendly as they conserve both energy and material[1]. It is necessary to synthesize new ternary, quaternary and quinary alloys with customized band gaps, lattice parameters and electron affinities in order to utilize more and more semiconductor materials in thin film solar cells[2]. Chalcopyrite based solar cells have recently shown promising results[3]. These materials exhibit good optical absorption quality; thus only a thin layer of material is required. The most important chalcopyrite compounds for solar cell applications are copper indium selenide ($CuInSe_2$), copper indium sulphide ($CuInS_2$), copper gallium selenide ($CuGaSe_2$) with a band gap of 1.0 eV, 1.5 eV and 1.7 eV respectively. The band gap can also be monitored by alloying with other elements e.g. copper–indium-gallium-selenide $Cu(In,Ga)Se_2$, latter known as CIGS, is obtained by the addition of Ga to the $CuInSe_2$ compound, which increases the band gap of the resultant material and hence known as CIGS solar cells. CIGS solar cells are the most economical among the various types of solar cell. Each layer has dissimilar physical and chemical properties and influences the overall efficiency of the device.

Copper Indium Gallium Selenide (CIGS) solar cells are known for their high efficiency and flexibility, making them promising candidates for thin-film photo-voltaics. In these cells, the buffer layer plays a critical role in facilitating efficient charge separation and transport between the CIGS absorber layer and the transparent conductive oxide (TCO) layer. In a hetero-junction solar cell buffer layer is mainly used to make a junction with the absorber layer[4]. Buffer layer is of paramount importance to obtain an optimum efficiency of a solar cell, as this layer is expected to decrease the mechanical stress that may exist between absorber layer and transparent front contact layer. Performance of thin film solar cells is affected by the thickness and quality of the buffer layer. Optimum thickness of buffer layer between the absorber layer and transparent conducting oxide (TCO) electrode is a basic requirement in the standard CIGS solar cell to improve its efficiency. These layers should be arranged in such a way so as to drive out the photo-generated carriers effectively and ensuring maximum amount of incident radiation to reach the junction. To improve the efficiency of the solar cell, use of semiconductor material having wide band gap for buffer

layer is one of the effective ways. It allows light energy from a broader region in the solar spectrum to pass through it so as to approach the absorber layer, which is the main problem in homo-junction solar cells. Furthermore, the recombination of carriers in the wide band gap semiconductor may be low. It is reported that buffer layer modifies the surface of the absorber layer via protection of the sensitive interface when window layer is deposited over it[5].The absorber and the buffer layers are made up of two different materials in hetero-junction solar cells and thus application of materials having different band gaps becomes possible. The risk from interface recombination is, however, higher for hetero-junction owing to the defects and the imperfections present at the junction. The use of buffer layer in combination with a suitable window layer can reduce the losses arising due to the recombination at the interface, which subsequently helps to obtain large band bending. From the above discussion, it is evident that the buffer layer should have large energy band gap in order to allow high optical transmittance in the visible range; so as to make most of the light to reach the absorber layer. It should be able to drive out the photo-generated carriers with minimum recombination losses. The band discontinuity between the buffer layer and the absorber layer must be designed in such a way that minority carriers do not face any band offset but there exist a large barrier for the majority carrier, which is achieved by using the materials with a large difference between their band gaps[6]. For growth consideration of epitaxial or highly oriented layers, lattice mismatch at the junction is also important. In the case of microcrystalline layers, mismatch varies spatially and thus the complicated effects, if any, is averaged out. While CdS has been the traditional buffer material due to its ideal band alignment with CIGS, concerns over toxicity and environmental impact have driven interest in ZnO-based alternatives[7].

The use of ZnO as a buffer layer in CIGS solar cells[8] offers a promising pathway to achieve high efficiency, environmental safety, and low-cost manufacturing**.** As research advances, ZnO-based buffer layers are becoming an attractive alternative to traditional CdS, contributing to the development of more sustainable and efficient thin-film solar technologies. The increased use of composite materials has broadened due to the reduced manufacturing costs as well as excellent performance. The development of the nano-composites in the form of core shell nanostructures has recently been attracting extensive interest. Coating of nano-particles to enhance their stability and dispersibility in solutions and to overcome the surface defects of nano-crystals may improve their optical properties. Attempts have been made in the present investigation to deposit ZnO thin films with and without silica using chemical bath deposition process and to compare the behaviour of these thin films in terms of their optical, structural and morphological attributes and hence to find the best possible combination which can further be exploited as a buffer layer in thin film solar cell. Silica has gained much attention in the recent past owing to its important properties namely high transparency for visible light, reduced electrical and thermal conductivity, low chemical activity and compatibility with ZnO[9].

Among the many different deposition techniques available to grow semiconductor thin films on different substrates, chemical bath deposition (CBD) is considered as the simplest one. The term CBD is, in general, used for the depositions from aqueous solutions where the desired product is chemically created and gets deposited physically in the same bath. It is a simple, flexible and effective approach to deposit large area thin films. By controlling the temperature, concentration, pH and complexing agent, the quality of films can be controlled. It is a template free technique and does not require expensive substrates such as Si wafer, GaN or Sapphire. In most of the cases no post annealing is required, so it allows possible usage of flexible polymer substrate. Now-a-days metal chalcogenide thin films are widely deposited by CBD. Under controlled precipitation conditions, a good deposition can be produced on suitable substrates during hydrolysis/condensation reactions[10]. It is an inexpensive technique as it does not require any sophisticated equipment and is performed at low temperature.

2. Materials and Methods

Deposition of ZnO and ZnO-SiO_2 thin films were carried out using a two step process: coating of ZnO seeds as described by Byrne D *et al*[11] on the ultra cleaned microscopic glass slides(2 x 2cm^2) procured from Blue Cross, India and further growth of thin films on the seeded substrates using AR grade chemicals procured from sigma Aldrich, without any further purification in the chemical bath. For pure ZnO thin films(sample code-Z) bath was prepared with aqueous solutions of "zinc nitrate hexahydrate ($Zn(NO_3)_2.6H_2O$)" and "Hexamethylenetetramine (HMTA) ($C_6H_{12}N_4$)" mixed together in equal volume as per the bath conditions mentioned in Table(1). For growth of ZnO-SiO_2 thin films a second bath was prepared with 0.5 ml of TEOS added to the aqueous solutions of "zinc nitrate hexahydrate ($Zn(NO_3)_2.6H_2O$)" and "Hexamethylenetetramine (HMTA) ($C_6H_{12}N_4$)" mixed together in equal volume as per the bath conditions mentioned in Table(1) for sample code-**S**. After the incubation period, the glass slides were rinsed with distilled water and then air dried. The optimized growth parameters (Table-1) were finalised on the basis of a detailed investigation and comparison of the optical, structural and electrical characterization of the samples prepared by varying pH, concentration and growth period[12,13,14].

The obtained ZnO and ZnO-SiO_2 thin films were further characterized for their optical properties through UV-visible spectroscopy, conducted in the wavelength regime of 250-800nm using UV-VIS Spectrophotometer (Model UV-2550) having integrated sphere assembly ISR 240A with a resolution of 1 nm. To investigate the morphology of the particles in thin films, all the thin films deposited were examined using scanning electron microscopy (SEM, HITACHI model S-3700N). Elemental phase compositions of deposited films were examined by energy dispersive X-ray spectroscopy (EDX). EDX system was integrated to SEM where the electron beam excites characteristic X-rays from the probed area. In order to examine the structural characteristics, X-ray studies were conducted. XPERT-PRO diffractometer (45 kV, 40 mA) equipped with a Gionometer PW3050/60 working with Cu K_α radiation of wavelength 1.5406 Å was used to record the XRD pattern. A Keithley source meter (model-2450) (SMU) was used to measure sheet resistance using four probe method.

3. Results and Discussion

It has been observed that use of TEOS as a surface modifier

helped in reducing the deposition time. During the deposition of ZnO thin films in acidic medium, HMTA acts as a chelating agent either through the slow decomposition of protonated hexamine[15] or may decompose into aldehyde and ammonia[16]. Ammonia generated in this process then combines with Zn^{2+} to produce a large number of zinc-aminocomplexes in the solution. On hydrolysis, these complexes form ZnO, which gets deposited on the glass substrate through a very slow decomposition reaction[17,18]. It has been observed that during the deposition process at acidic pH, precursor solution remained transparent throughout the growth period due to slow hydrolysis of HMTA. Similar findings were also reported by Govender *et al*[19] who observed that at pH 5.0 no precipitation occurred in the baths and dissolution of the nanocrystalline ZnO template layer occurred. By using TEOS along with HMTA in the basic bath, thin and uniform films were obtained at faster rate as compared to acidic pH. TEOS is an alkoxysilane with four alkoxyl groups. A group will be hydrolyzed and reacts with the OH^- group on the hydroxylated ZnO surface under basic conditions. Due to faster hydrolysis; branched clusters are formed and result in the formation of ZnO-SiO_2 composite. Also above pH value of 5, the negative charge on silica increases rapidly. This leads to an electrostatic interaction with positively charged ZnO, resulting in uniform composite films. Film thickness of about 481 nm could be attained within 20 minute as compared to 535 nm thickness of pure ZnO thin films in 1hour at a pH of 5.0.

Following sections deal with the comparison of the optical parameters, structural, morphological and electrical attributes of sample **S** and sample **Z** in order to understand the effect of addition of silica on these properties and to justify the use of ZnO-SiO_2 film in the thin film CIGS solar cell.

3.1 Reaction Mechanism of pure ZnO

$HMTA(CH_2)_6N_4$) was used as a complexing agent and Zn $(NO_3)_2.6H_2O$ provided Zn^{2+} ions required for building up ZnO nano-structures. The presence of HMTA avoided the rapid precipitation of zinc hydroxide and allowed a stable dispersion to be formed. It acted as a weak base and also as a pH buffer during the film deposition[19]. HMTA is non-ionic tetradentate cyclic tertiary amine with a high solubility in water, and gradually hydrolyzes in the aqueous solution at a slow rate to produce ammonia (NH_3) and formaldehyde (HCHO) under appropriate thermal conditions. NH_3 plays two important roles:

(i) It produces a basic environment by producing NH_4^+ and OH^- ions, which are necessary for the production of $Zn(OH)_2$. The chemical reactions can be summarized as follows[17].

$(CH_2)_6N_4 + 6H_2O \rightarrow 6HCHO + 4NH_3$

$NH_3 + H_2O \rightarrow NH_4OH \rightarrow NH_4^+ + OH^-$

$2OH^- + Zn^{2+} \rightarrow Zn(OH)_2$

$Zn(OH)_2 \rightarrow ZnO + H_2O$

(ii) Secondly, it coordinates with the Zn^{2+}ions to produce zinc ammonia complex. Slow hydrolysis is important because if HMTA hydrolyzes rapidly and produces a large amount of OH^-, resulting in quick precipitation of Zn^{2+}ions in the solution due to high pH. As the reaction proceeds, Zn^{2+} ions are gradually consumed and decomposition of zinc-ammonia complex occurs slowly, resulting a very low level of super-saturation in the solution and thereby stabilize the concentration of Zn^{2+} ions. So, controlling the pH and concentration of Zn^{2+} ions promotes heterogeneous growth over homogeneous growth by avoiding a high ZnO saturation index. Zn $(OH)_2$ dehydrates into ZnO. The reaction mechanism can be summed up as[18].

$Zn(NO_3)_7 \rightarrow Zn^{2+} + NO_3^-$

$C_6H_{12}N_4 + 10H_2O \rightarrow 6HCHO + 4NH_3H_2O$

$Zn^{2+} + 4NH_3.H_2O \rightarrow [Zn(NH_3)_4]^{2+} + 4H_2O$

$[Zn(NH_3)_4]^{2+} + 4H_2O \rightarrow Zn(OH)_2 + 4\,[NH_4]^{2+} + 2OH^-$

$Zn(OH)_2 \rightarrow ZnO + H_2O$

During the precipitation, the formation of a solid phase should start in the solution when ionic product (I_p) exceeds the solubility product (k_{ps}) which depends upon the pH of the solution[20]. Since the solubility product for Zn $(OH)_2$ is 10^{-17}, under basic pH 10.8 due to higher reaction rate, Zn $(OH)_2$ precipitates very fast. This resulted in comparatively thicker films with less transmittance. Tada[15] reported that hydrolytic decomposition of protonated hexamine $[(CH_2)_6N_4H]^+$takes place under acidic conditions, thereby producing protonated ammonia through the following reaction in the chemical bath:

$[(CH_2)_6N_4] + H^+ \rightarrow [(CH_2)_6N_4H]^+$

$[(CH_2)_6N_4H]^+ + 3H^+ + 4NO_3^- + 6H_2O \rightarrow 4NH_4^+ + 4NO_3^- + 6CH_2$

Under weak acidic conditions, ammonia combines with Zn^{2+} ions and produces zinc-amino complexes in enormous number in the solution. These complexes were hydrolyzed directly to form ZnO through the decomposition reaction on the substrate and on the inner surface of the vessel. Hence, ammonia could stabilize Zn^{2+}ions through reversible reaction of creating and decomposing of zinc-ammonia complex. It was observed that in acidic bath (pH=5) the solution remained transparent during deposition indicating a slow chemical deposition process. As a result thin films deposited at this pH exhibited higher transmittance. Due to slow and controlled precipitation, short range grain size[21] calculated using Brus equation was found to be quite small owing to a blue shift in the band-edge at this pH.

3.2 Reaction Mechanism of ZnO-SiO_2 nano-composite thin film

The hydrolysis rate of TEOS was accelerated with variation in pH and also due to the presence of ammonia released in the bath during decomposition of HMTA in the bath. Ammonia acts as a catalyst also besides controlling Zn^{2+} ion concentration. At alkaline pH, Zn^{2+} may exist in a series of intermediates and ZnO may be obtained by the dehydration of these intermediates and due to the presence of OH^-, ZnO is hydroxylated. Similar observations were reported by Xu[18].

$Zn^{2+} + 2\,OH^- \leftrightarrow Zn(OH)_2$

$Zn(OH)_2 + 2\,OH^- \leftrightarrow [Zn(OH)_4]^{2-}$

$[Zn(OH)_4]^{2-} \leftrightarrow ZnO_2^{2-} + 2H_2O$

$ZnO_2^{2-} + H_2O \leftrightarrow ZnO + 2\,OH^-$

$ZnO + 2OH^- \leftrightarrow ZnOOH^-$

TEOS is an alkoxy silane with four alkoxyl groups[22]. An alkoxyl group will be hydrolyzed and react with the OH^- group on the hydroxylated ZnO surface under basic

conditions, due to faster hydrolysis, branched clustered are formed and results in the formation of ZnO-SiO_2 composite (Figure 1).

3.3 Effect of Silica on the Optical Properties of ZnO

To find out how the optical properties of ZnO are modified by the addition of silica, the optical properties of ZnO-SiO_2 (Sample–S) are compared with pure ZnO thin films (Sample–Z). The comparative results are summarized in Table 2 and Figures 2-8.

3.3.1 Transmittance

It has been observed that addition of silica improved the optical characteristics of ZnO in the visible region. The transmittance of sample **S** is observed to be higher (95%) as compared to that of sample **Z** (92.9%) (Figure 2).

3.3.2 Absorption coefficient

Figure 3 shows the variation of absorption coefficient with wavelength for samples Z and S. The absorption coefficient of sample S was observed to be $0.105x10^6$/m as compared to $0.137x10^6$/m for sample **Z** thin films. However both of them are constant in the visible region.

3.3.3 Band Gap

The optical band gap was determined by extrapolating downward the corresponding straight line portions of the graphs between $(\alpha h\nu)^2$ and the photon energy hν, till the intersection with the energy axis[23,24] as shown in Figures 4(a) and Figure 4(b). A blue shift as compared to the bulk ZnO (3.37 eV) was observed in the band gaps of both the samples. Band gap of sample **S** exhibited band gap value of 4.01eV whereas sample **Z** has 4.10 eV.

3.3.4 Crystallite Size

The short range grain sizes have been calculated using Brus equation[25] based on "Effective Mass Approximation" (EMA) and were found to be 1.70 nm and 1.79 nm corresponding to samples **Z** and **S** respectively.

The smoothness with reduced thickness of ZnO-SiO_2 nano-composite thin films might be responsible for its improved transmittance although the band gap observed in the thin film of ZnO was slightly more.

3.3.5 Extinction coefficient

The extinction coefficient remained almost constant in the visible region for sample **S**. However, it increases with the increase in wavelength for **Z** (Figure 5). Its value at wavelength 500nm was observed to be 0.0039 for sample **S** and 0.0054 for sample **Z**. Thus the lower value of extinction coefficient of sample **S** indicated that with the addition of silica, the extent of absorption loss of the incident photon energy decreases.

3.3.6 Refractive Index

The refractive index for sample **S** is observed to be 1.38 whereas it is 1.48 for sample **Z** at wavelength of 500nm (Figure 6). It is concluded that addition of silica lowers the refractive index. At higher wavelengths, a further decrease in the refractive index of composite film was observed.

3.3.7 Dielectric Constant

For sample **S** the value of ε_r was observed to be 1.93 as compared to 2.20 for sample Z **(**Figure 7). Lowering of the dielectric constant of the material for buffer layer is expected to increase the efficiency of solar cell.

3.3.8 Optical Conductivity

The numerical value of optical conductivity of sample **S** was $0.034x10^{14}$ /sec which was smaller as compared to sample **Z** ($0.048\ x10^{14}$ /sec) at wavelength of 500 nm (Figure 8). There is a sharp increase in optical conductivity due to high absorbance in thin films at higher energies and is almost constant in the visible region.

4. Effect of Silica on the structural and Morphological Properties of ZnO

To study the influence of silica on the structure and morphology of ZnO thin films of respective samples were compared for their X-Ray diffraction spectra and SEM micrographs.

4.1 X-Ray diffraction spectra

X-Ray diffraction patterns as shown in Figure 9(a) and Figure 9(b) reveal that both the samples are amorphous in nature.

4.2. SEM Analysis

Figure 10 exhibits a sheet type dense film on the glass substrate for ZnO-SiO_2 nano composite thin film (Sample-**S**), whereas scattered flakes were visible on the substrate for ZnO thin film (Sample-**Z**). These micrographs clearly show that material coverage in case of ZnO modified by silica was much improved as compared to pure ZnO that too in a smaller growth period. EDX spectra (Figures 11) indicate that ZnO-SiO_2 nano composite thin film (Sample-**S**) and ZnO thin films(Sample –Z) are pure as manifested by the absence of impurity peaks. However, the presence of a small peak of silica in sample **Z** may be attributed to the substrate material.

5. Effect of Silica on Electrical Properties of ZnO

Sample **Z** exhibited a higher value ($8.1x10^8\Omega$/square) of the sheet resistance than that for Sample S($2.958x10^8\Omega$/square). The higher sheet resistance of ZnO thin films as compared to ZnO-SiO_2 nanocomposite thin film may be attributed to the discontinuous nature of sample **Z** as revealed by SEM micrograph(Figure 10)

6. Conclusions

Comparison of the physical, optical and electrical parameters of ZnO-SiO_2 nano-composite thin film with ZnO as presented in Table 2, revealed that composite thin film resulted in an optimum combination of optical and morphological characteristics. The material coverage on the substrate was increased due to the addition of silica. Within shortest time, it was possible to deposit continuous thin films without any further heat treatment, with less material requirement and better physical and optical properties in the form of ZnO-SiO_2 thin film. The ability to control physical properties and optical characteristics of ZnO thin films like transmittance, absorption coefficient, extinction coefficient, dielectric constant, optical conductivity etc. by the addition of TEOS demonstrated that use of the polymer(TEOS), while taking the advantage of other cumulative effects of growth parameters such as the temperature, pH value and the concentration enhances the possibilities for the controlled synthesis of inorganic crystals with well-defined shape, size and uniform structure thereby allowing an

oriented approach to fabricate economical ZnO based thin films for further use in solar cell devices as a buffer layer. Improved optical and morphological properties shown by sample **S** as compared to sample **Z** revealed that as deposited ZnO-SiO_2 film are economical in terms of time and quantity of material. Silica helped in modifying the electronic structure and surface states of ZnO, which can be utilized for tailoring materials for specific applications, such as in solar cells, optoelectronics, UV shielding, or photo catalysis.

References

[1] Chopra, K. L., Paulson, P. D., Dutta, V., 2004," Thin Film Solar cells: An Over View," Prog. Photovolt: Res., 12, pp. 69-92.

[2] Chopra, K. L., and Kaur, I., 1983," Thin Film Device Applications," Newyork: Plenum Press, pp. 106-108.

[3] Ramanathan, K., Keane, J., Noufi, R., 2005, " Properties of High-Efficiency CIGS Thin-Film Solar Cells," 31st IEEE Photovoltaics Specialists Conference and Exhibition. Lake Buena Vista, Florida.:1-7.

[4] Mccandless, B. E. and Hegedus, S. S.,1991, " Influence of CdS window layer on thin-film CdS/CdTe solar cell performance". Proceedings of the 22nd IEEE Photovoltaic Specialists Conference, pp. 967-972.

[5] Sterner, J., 2004 "ALD Buffer Layer Growth and Interface Formation on Cu(In,Ga)Se_2 Solar Cell Absorbers". Comprehensive Summaries of Uppsala Dissertations from the Faculty of Science and Technology, 942, pp.1-52.

[6] Niemegeers, A., and Burgleman, M. and De Vos, A.,1995, "On the CdS/$CuInSe_2$ Conduction Band Discontinuity," Appl. Phys. Lett., 67(6):843-5.

[7] Rana, T.R., Kim, S. Y., Kim J. H., Kim, K. and Yun, J. H., 2017, "A Cd-reduced hybrid buffer layer of CdS/Zn(O,S) for environmentally friendly CIGS solar cells," Sustainable Energy & Fuels, 1, pp. 1981-1990.

[8] Törndahl,T., Hultqvist, A., Platzer-Björkman, C., and Edoff M., 2010,"Growth and characterization of ZnO-based buffer layers for CIGS solar cells", Proc. SPIE 7603, Oxide-based Materials and Devices, 76030D.

[9] Yang, Y., Li, Y. Q., Shi, H. Q., Li, W. N., Xiao, H. M., Zhu, L. P. *et al.* ,2011, " Fabrication and characterization of transparent ZnO-SiO_2/silicone nanocomposites with tunable emission colors ," Composites: Part B, 42, pp. 2105-10.

[10] O'Brien, P. and McAleese, J., 1998, "Developing an understanding of the processes controlling the chemical bath deposition of ZnS and CdS," J. Mater. Chem, 8(11), pp. 2309-14.

[11] Byrne, D., McGlyn, E., Cullin J., and Henry, M. O., 2011, "A catalyst-free and facile route to periodically ordered and c-axis aligned ZnO arrays on diverse substrates," Nanoscale,3**,** pp. 1675-1682.

[12] Kumar,S., Jeon, H.C., Kang, T.W., Seth R. et. al.,2019, " Variation in chemical bath pH and the corresponding precursor concentration for optimizing the optical, structural and morphological properties of ZnO thin films," Journal of Materials Science: Materials in Electronics,30, pp.17747-17758.

[13] Seth, R., Panwar, S., Kumar, S., Kang, T. W., and Jeon, H. C., 2017, "pH Dependent Studies of Chemical Bath Deposition Grown ZnO-SiO2 Core-Shell Thin Films," Journal of the Korean Physical Society, 70(1), pp.98-103.

[14] Seth, R.,2018, "Physical Properties of CBD Based ZnO-SiO_2 Core-Shell Composite Thin Films," IJISET,5(12), pp.130-136.

[15] Tada H. 1960, "Decomposition Reaction of Hexamine by Acid," J. Am. Chem. Soc., 82(2), pp. 255-263.

[16] Xu, S., Lao, C., Weintraub, B., Wang, Z. L.,2008, "Density controlled growth of aligned ZnO nanowire arrays by seedless chemical approach on smooth surfaces," J. Mater. Res., 23, pp. 2072-77.

[17] Ladanov, M., Ram, M. K., Matthew, S. G. and Kumar, A.,2011, "Structure and opto-electrochemical properties of ZnO nanowires grown on n-Si substrate," Langmuir, 27(14), 9012–9017.

[18] Xu, S. and Zhong, L. W., 2011, "One dimensional ZnO Nanostructures: Solution Growth and Functional Properties," NanoRes.,4(11), pp. 1013-1098.

[19] Govender, K., David, S. B., Kenway, P. B., and O'Brien, P., 2004, "Understanding the factors that govern the deposition and morphology of thin films of ZnO from aqueous solution," J. Mater. Chem.,14, pp.2575-2591.

[20] Lopez, M. O., Avila-Garcia, A., Albor-Aguilera, M. L.,2003, "Sanchez-Resendiz VM. Improved efficiency of the chemical bath deposition method during growth of ZnO thin films," Materials Research Bulletin, 38, pp.1241-1248.

[21] Chakrabarti, S., Ganguli, D., Chaudhuri, S., 2004, "Excitonic and defect related transitions in ZnO-SiO_2 nanocomposites synthesized by sol-gel technique," phys.stat.sol.(a), 201(9), pp.2134-2142.

[22] Wu, Y. L., Tok, A.I.Y., Boey F.Y.C., Zeng, X. T., Zhang, X. H.,2007, "Surface modification of ZnO nanocrystals," Applied Surface Science, 253,pp. 5473-5479.

[23] Tauc, J., 1974, Amorphous and Liquid Semiconductors. Newyork:Platinum Press;1974.p-159.

[24] Pankove, J. I.,1971, Optical Process in Semiconductors. Prantice Hall, New Jersey, pp. 34-35.

[25] Brus, L. E., 1984,"Electron-Electron and Electron-Hole Interactions in Small Semiconductor Crystallites: The Size Dependence of the Lowest Excited Electronic State," Journal of Chemical Physics, 80(9), pp.4403-4409.

Sample code	$Zn(NO_3)$ Conc.	HMTA Conc.	TEOS	pH	Deposition Time(min)	Deposition	Temp(^{0}C)
Z	100mM	100mM	-	5.0	60	90	
S	100mM	100mM	0.5 ml	10.8	20	90	

Table 1: Optimized growth parameters for the deposition of ZnO and ZnO-SiO_2 thin films

Sample Code	Thickness	Transmittance (%)	AbsorptionCoeff. ($\alpha X10^6 m^{-1}$)	nd Gap(E_g) (eV)	ystallite Size (nm)	inction Coeff.	Refractive Index	Dielectric Constant	Opt. Con/Sec $X10^{14}$	Sheet Res $x10^8$ (Ω /Square)
S	481nm	95	0.105	4.01	1.79	0.0039	1.38	1.93	0.034	2.958
Z	535 nm	92.9	0.137	4.10	1.70	0.0054	1.48	2.19	0.048	8.1

Table 2: Comparison of Physical Properties of ZnO and ZnO- SiO_2 nano-composite thin films.

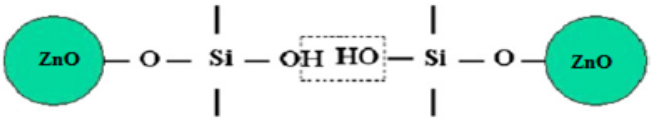

Figure 1 Mechanism of ZnO-SiO_2nano composite formation.

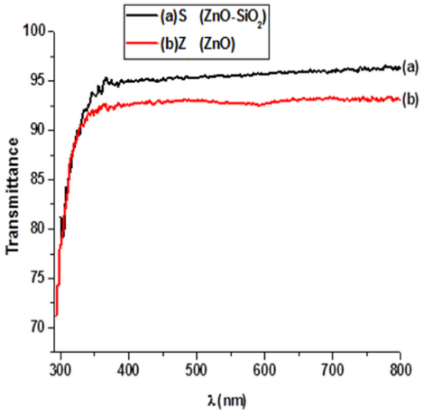

Figure 2: Transmittance

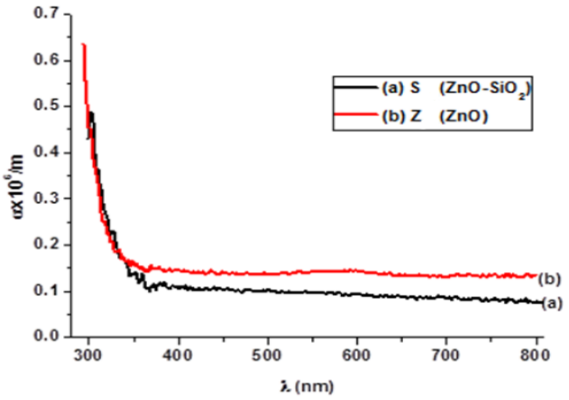

Figure 3. Absorption Coefficients

.

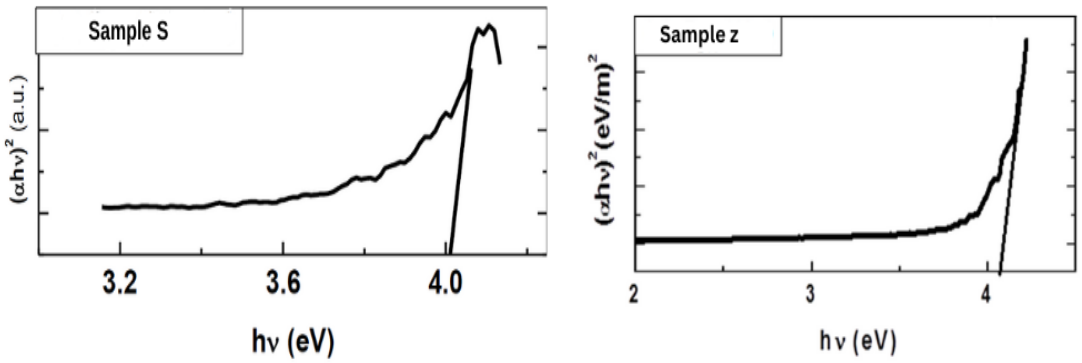

4(a) 4(b)

Figure 4. Band Gap of (a) ZnO-SiO_2 nanocomposite thin film (b) ZnO thin film.

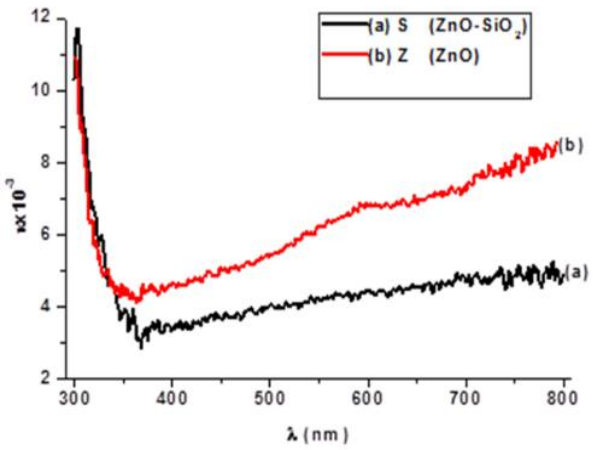

Figure 5. Extinction Coefficient

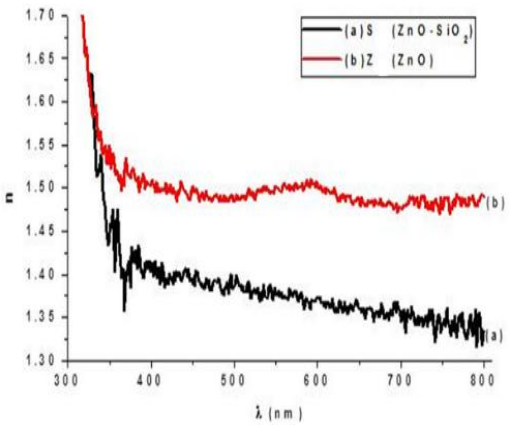

Figure 6. Refractive Indices

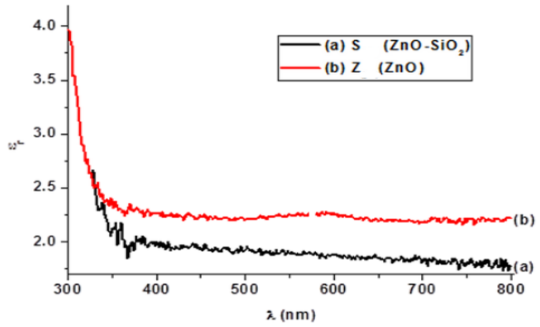

Figure 7. Dielectric Constant

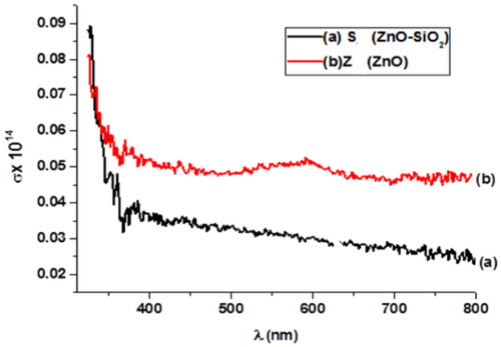

Figure 8. Optical Conductivity

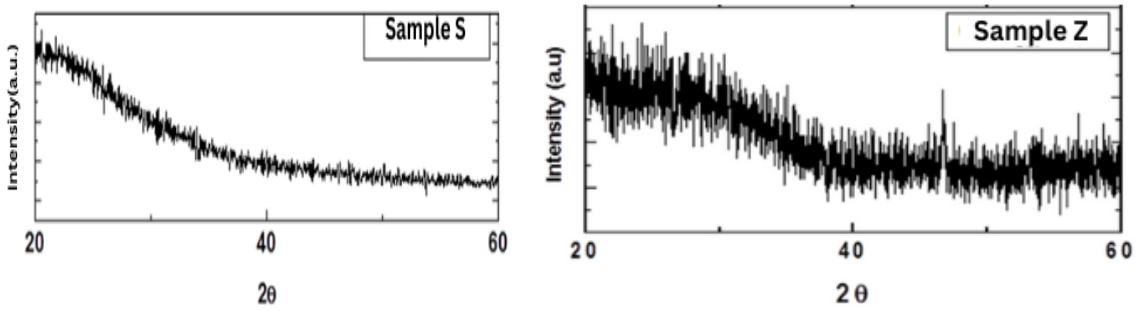

Figure 9 X-Ray diffraction spectra of ZnO-SiO_2 nanocomposite thin film and ZnO thin film.

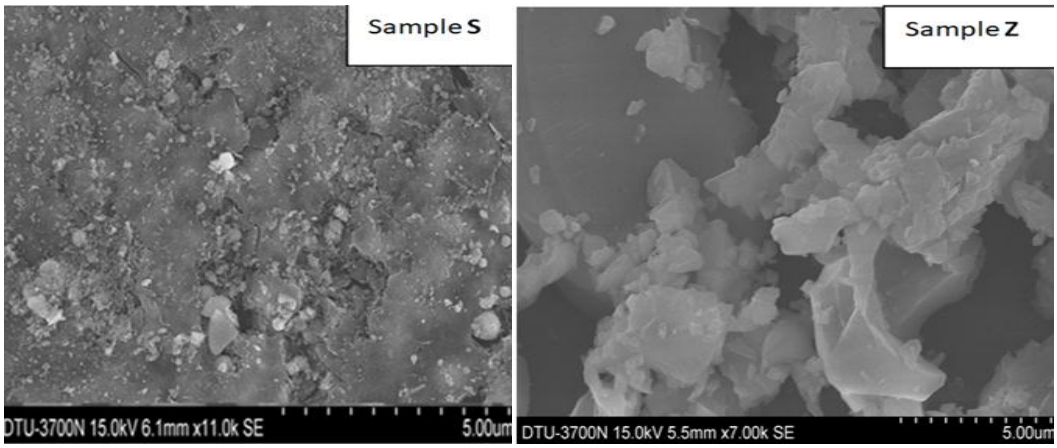

Figure 10. SEM images of (a) ZnO-SiO_2 nano-composite thin film (b) ZnO thin film.

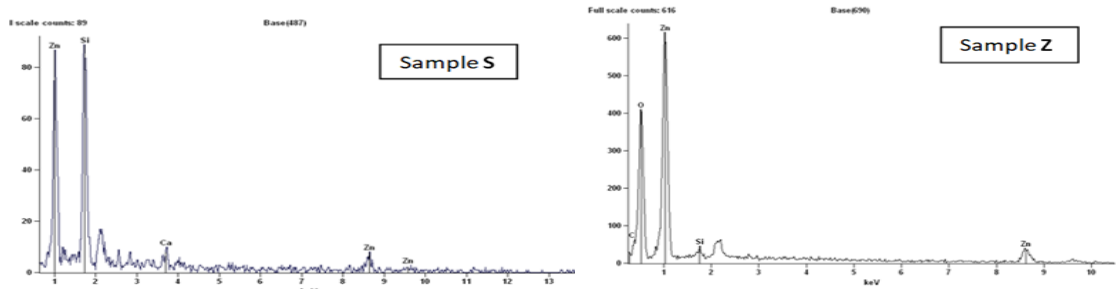

Element Line	Net Counts	Int. Cps/nA	Weight %	Weight % Error	Atom %	Atom % Error	Formula	Standard Name
O K	502	---	33.01	+/-1.45	55.46	+/-2.43	O	
Si K	922	---	29.27	+/-1.14	28.01	+/-1.09	Si	
Si L	0	---	---	---	---	---		
Ca K	74	---	3.93	+/-0.58	2.64	+/-0.39	Ca	
Ca L	0	---	---	---	---	---		
Zn K	71	---	33.80	+/-7.14	13.90	+/-2.94	Zn	
Zn L	791	---	---	---	---	---		
Total			100.00		100.00			

Element Line	Net Counts	Int. Cps/nA	Weight %	Weight % Error	Atom %	Atom % Error	Formula	Standard Name
C K	0	---	0.00	---	0.00	+/-0.00	C	
O K	3547	---	36.56	+/-0.68	69.37	+/-1.29	O	
Si K	261	---	1.90	+/-0.27	2.05	+/-0.29	Si	
Si L	0	---	---	---	---	---		
Zn K	670	---	61.54	+/-4.04	28.57	+/-1.88	Zn	
Zn L	7038	---	---	---	---	---		
Total			100.00		100.00			

Figure 11. EDX Spectra of (a) ZnO-SiO_2 nano-composite thin film (b) ZnO thin film.